5-11-2016

A Scalable Strategy for Open Loop Magnetic Control of Microrobots Using Critical Points

Luis Guerrero-Bonilla
University of Pennsylvania, luisg@seas.upenn.edu

Subhrajit Bhattacharya
University of Pennsylvania, subhrabh@math.upenn.edu

Vijay Kumar
University of Pennsylvania, kumar@seas.upenn.edu

A Scalable Strategy for Open Loop Magnetic Control of Microrobots Using Critical Points

Abstract
A novel scalable strategy for open loop control of ferromagnetic microrobots on a plane using a scalable array of electromagnets is presented. Instead of controlling the microrobot directly, we create equilibrium points in the magnetic force field that are stable and attractive on the plane in which the microrobot is to be controlled. The microrobot moves into these equilibrium points rapidly in presence of low viscous forces, and thus controlling the equilibrium points let us control the microrobot precisely. An unit/cell in the array of electromagnets allows precise control of the microrobot in the unit/cell's domain. Motion synthesis across multiple overlapping domains allows control of the microrobot in large regions across the array. We perform numerical analysis and demonstrate the control of the ferromagnetic microrobot using the proposed method through simulations.

Keywords
Microrobotics, Magnetic Control

Disciplines
Applied Mechanics | Engineering | Mechanical Engineering

A Scalable Strategy for Open Loop Magnetic Control of Microrobots Using Critical Points

Luis Guerrero-Bonilla[1], Subhrajit Bhattacharya[1] and Vijay Kumar[1]

Abstract— **A novel scalable strategy for open loop control of ferromagnetic microrobots on a plane using a scalable array of electromagnets is presented. Instead of controlling the microrobot directly, we create equilibrium points in the magnetic force field that are stable and attractive on the plane in which the microrobot is to be controlled. The microrobot moves into these equilibrium points rapidly in presence of low viscous forces, and thus controlling the equilibrium points let us control the microrobot precisely. An unit/cell in the array of electromagnets allows precise control of the microrobot in the unit/cell's domain. Motion synthesis across multiple overlapping domains allows control of the microrobot in large regions across the array. We perform numerical analysis and demonstrate the control of the ferromagnetic microrobot using the proposed method through simulations.**

I. INTRODUCTION AND PROBLEM STATEMENT

In recent years there has been significant interest in the design and control of microrobots. Typically these are sub-millimeter scale particles requiring precise motion control. Precision control of such microrobots has vast applications in various areas of medicine such as cell manipulation [16], precision micro-surgery and targeted drug delivery [8], [5]. The primary challenge behind developing such a system is however the difficulty in actuation and control at the sub-millimeter scales. Typically this is achieved using some form of external actuation.

Micro-bio robots (MBRs), for example, are microstructures with attached flagellated bacteria, which can be controlled by intermittently exciting or inhibiting the bacteria using electric fields [14], [10], magnetic fields [12] or UV light [15]. However, using biological systems, such as bacteria, as the instrument for controlling microrobots has the disadvantages of being unreliable, difficult to manufacture, model and control, and unsuitable for use in applications such as medicine and surgery.

The alternative, and unsurprisingly widely studied, method for controlling microrobots is to use external fields, in particular electromagnetic fields. Pure electric fields have been used to control charged colloidal particles [4] using electrokinetic transport mechanisms. More commonly, magnetic fields are used to manipulate microrobots since magnetic fields are easy to create and manipulate using electromagnetic coils [5], [11], [13], [7]. While a variety of strategies have been proposed, all the current methods in literature attempt to control the instantaneous acceleration of the robot by manipulating the force field due to the interaction of the magnetic field with the robot's magnetic moment. In a low Reynolds number system this allows quasi-static control of the microrobot when the viscous forces are significantly higher than the inertial forces. This strategy requires a feedback loop (usually through a camera) that would allow control of the magnetic field (and its gradients) in a desired way at the current location of the microrobot. The number of magnets requires for achieving such controllability of the magnetic field at arbitrary points in space has been determined [11], and the approach has even been used to control multiple microrobots [1], [9], [2].

However, a major drawback of the aforesaid strategy is that a precise control of the microrobot requires that the robot be slow-moving and there be a high frequency feedback loop. Since the robot is moving under the influence of a non-zero force all the time, a fast-moving microrobot may be difficult to control in high Reynolds number environments. Although critical points (or static equilibrium points – points of zero force) are typically present in the force field, very often those can be unstable or saddle, and bifurcations in the critical points has made the past literature to mostly avoid the critical points when addressing the problem of microrobot control, rather than exploiting them. In this paper we tackle that very problem head-on, and propose a method for controlling the micro-robots by exploiting the critical points. Instead of trying to compute the coil currents that would generate the magnetic field for the required acceleration/force at the instantaneous position of the microrobot, we propose the creation a stable critical point at the desired position of the microrobot. If the microrobot is within the basin of attraction of the stable critical point, it will move to and stabilize at that position. It is particularly beneficial in relatively high Reynolds number situations where the microrobot can be fast moving. In addition, this approach allows us to reliably move the microrobot without relying on a high-frequency feedback.

Due to the Earnshaw's theorem for magnetic fields [6], it is actually impossible to create a stable critical point in the 3-dimensional Euclidean space for the force acting on a ferro-magnetic microrobot. However, if the microrobot is constrained to move along a plane, it is completely possible to have a critical point on the plane that is stable along the plane. In this paper we thus consider the microrobot to be constrained to move on a plane. Manipulation of particles using stable manifolds and limit cycles in force fields induced by magnetic fields is not a new idea. In fact magnetic levitation and control of plasma in particle accelerators is based on similar principles. In those cases, however, either

[1]GRASP Laboratory, School of Engineering and Applied Sciences, University of Pennsylvania, Philadelphia, PA 19104, U.S.A. luisg, kumar@seas.upenn.edu, subhrabh@math.upenn.edu

super-conducting materials are used to create spatial stable equilibrium or the particles are constrained to move in a limit cycle rather than stabilizing in a critical point. We believe that within the microrobotics community this is the first time that this idea is being used for manipulating and precisely controlling ferromagnetic microrobots.

The paper is organized as follows. Section II describes the forces on what will be considered a microrobot due to its interaction with a magnetic field. Section III describes the selected coil arrangement and the strategy to manipulate the currents in each coil. . Section IV shows experiments and results. Section V has the conclusions and future work.

II. Forces on a Microrobot in a Magnetic Field

A. Theory

The components of the magnetic field $\mathbf{B}_i$ created by a single coil of radius R with current I_i centered at the origin are given by

$$B_{xi} = \frac{\mu_0 I_i R}{4\pi} \int_0^{2\pi} \frac{z \cos\theta d\theta}{\left[(x - R\cos\theta)^2 + (y - R\sin\theta)^2 + z^2\right]^{\frac{3}{2}}} \tag{1}$$

$$B_{yi} = \frac{\mu_0 I_i R}{4\pi} \int_0^{2\pi} \frac{z \sin\theta d\theta}{\left[(x - R\cos\theta)^2 + (y - R\sin\theta)^2 + z^2\right]^{\frac{3}{2}}} \tag{2}$$

$$B_{zi} = \frac{\mu_0 I_i R}{4\pi} \int_0^{2\pi} \frac{(R - x\cos\theta - y\cos\theta)\, d\theta}{\left[(x - R\cos\theta)^2 + (y - R\sin\theta)^2 + z^2\right]^{\frac{3}{2}}} \tag{3}$$

where μ_0 is the permitivity constant of air, I_i is the current through the coil i, x,y and z are the coordinates at the point in space where the equations give the value of the field. A reference to the theory behind this equations is [6] . An example of the magnetic field produced by a single coil is shown in Fig. 1.

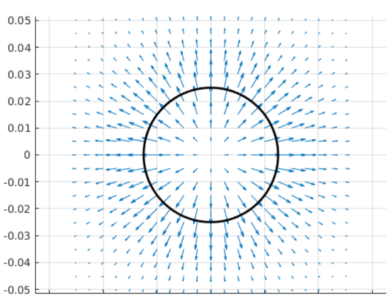

Fig. 1. Magnetic field of a circular coil of radius 0.025 m centered at the origin, on a plane 0.02 m above the plane of the coil. The current is 0.02 A flowing counterclockwise.

For the purposes of this paper, a microrobot will be modeled after a particle with a magnetic dipole moment $\mathbf{m}$ of constant magnitude m. Assume that there is a magnetic field $\mathbf{B}$ in the surrounding space. Then, the force on the microrobot is given by

$$\mathbf{F} = \nabla(\mathbf{m} \cdot \mathbf{B}) \tag{4}$$

To simplify our analysis, we will assume that the dipole moment of the particle orients itself instantaneously in the direction of $\mathbf{B}$, so that

$$\mathbf{F} = m\nabla(\|\mathbf{B}\|) \tag{5}$$

An example of the force field described by equation (5) is shown in Fig. 2.

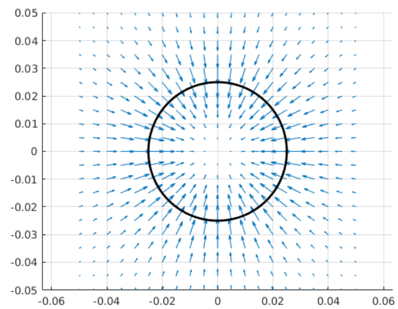

Fig. 2. Force field of a circular coil of radius 0.025 m centered at the origin, on a plane 0.02 m above the plane of the coil, acting on a dipole moment of magnitude m at different locations on the plane. The current is 0.02 A flowing counterclockwise.

The total force on the microrobot is calculated by adding the magnetic fields of each coil in the arrangement, such that $\mathbf{B} = \sum_i^n \mathbf{B}_i$. To analyze the stability of these equilibrium points, we calculate the Hessian matrix

$$H = \begin{bmatrix} \frac{\partial F_x}{\partial x} & \frac{\partial F_x}{\partial y} \\ \frac{\partial F_y}{\partial x} & \frac{\partial F_y}{\partial y} \end{bmatrix} \tag{6}$$

and select the currents that make both eigenvalues of H negative.

B. Numerical method

The gradient of $\mathbf{B}$ can be expressed in terms of integrals using Leibniz's rule, and since the integrals and its derivatives are only functions of the variables θ, x, y and z, the integrals can be evaluated numerically at any desired position in space to express the force as polynomials in the currents I_i.

$$\nabla(\|\mathbf{B}\|) = \frac{1}{\|\mathbf{B}\|} \begin{bmatrix} B_x \frac{\partial B_x}{\partial x} + B_y \frac{\partial B_y}{\partial x} + B_z \frac{\partial B_z}{\partial x} \\ B_x \frac{\partial B_x}{\partial y} + B_y \frac{\partial B_y}{\partial y} + B_z \frac{\partial B_z}{\partial y} \\ B_x \frac{\partial B_x}{\partial z} + B_y \frac{\partial B_y}{\partial z} + B_z \frac{\partial B_z}{\partial z} \end{bmatrix} \tag{7}$$

To solve the integrals numerically, we used MATLAB's ode45 function. The necessary currents to obtain static equilibrium points can be obtained by solving $\mathbf{F} = \mathbf{0}$ using methods such as [3].

III. COIL ARRANGEMENT AND CURRENT MANIPULATION

Diverse arrangements for coils were simulated. The selected arrangement in this paper to show the idea behind the position control strategy is shown in Fig. 3.

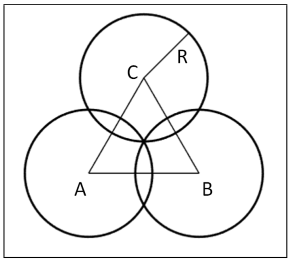

Fig. 3. Coil arrangement

where the circles represent coils each of radius R. The plane on which the microrobot lies is parallel to the plane of the coils and at a distance z_p above it. This arrangement allows to create stable static equilibrium points within the triangle ABC, and it is easily scalable, as we discuss next.
The triangle ABC can be broken into sections as shown in Fig. 4. Because of the symmetry, it is only required to analyze one of the sections to obtain the necessary currents to create stable equilibrium points in it.

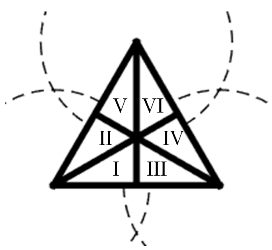

Fig. 4. Sections I to VI of the triangle connecting the center of each coil.

Let us label the coils the same as the location of their centers, A, B and C, and let current I_1 flow through coil A, I_2 through coil B and I_3 through coil C. Consider now a sampling of section I, as shown in Fig. 5

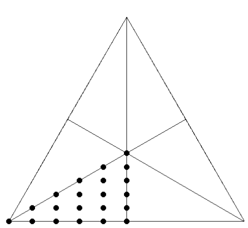

Fig. 5. A sampling of section I.

Let I_1 be the constant value I_1^*. The values of I_2 and I_3 to obtain a stable static equilibrium at the sampled positions (x, y) can be solved for. Call these values I_{2xy}^* and I_{3xy}^* respectively. Fig. 6 shows such an equilibrium in section I.

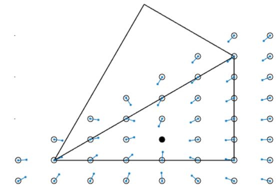

Fig. 6. A cualitative depiction of a stable static equilibrium in section I and the force field surrounding it.

Section	Transform position to Section I by...
I	Applying identity operator
II	Reflect on $y - x\tan\frac{\pi}{6}$
III	Reflect on $x = 0$
IV	Rotate on the z axis by $-\frac{\pi}{3}$
V	Rotate on the z axis by $\frac{\pi}{3}$
VI	Reflect on $y + x\tan\frac{\pi}{6}$

TABLE II

POSITIONS ON SECTION II TO VI HAVE TO BE TRANSFORMED TO SECTION I TO USE THE CORRESPONDING CURRENTS.

Based on the currents obtained in section I, it is possible to infer the currents to create the equilibrium points at the relative same locations in the other sections. To do this, desired position in any section can be transformed to section I by reflecting or rotating the coordinates. As an example, Fig. 7 shows a static stable equilibrium in section II at the position obtained by reflecting the equilibrium point on section I shown in Fig. 6 on the line $y = \tan\frac{\pi}{6}x$ or, had it been desired to located in some other position in section II, by reflecting such a position into section I and obtaining the necessary currents to create it in section I. In section II however, while I_1 stays the same, the roles of I_2 and I_3 are interchanged: $I_2 = I_{3xy}^*$ and $I_3 = I_{2xy}^*$. Table I and Table II summarize how to transform positions and select currents among the sections of the triangle, using section I as reference. This symmetry can be exploited twofold: It is enough to analyze one section of the triangle for the identification of the parameters of the system, and obtaining experimental data of points in one section gives the current information for the corresponding point in a different section.

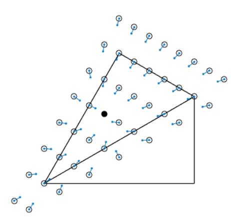

Fig. 7. A cualitative depiction of a stable static equilibrium in section II and the force field surrounding it.

For a given position, the solution for currents that create a static stable equilibrium point is not unique. The currents to apply are selected so that the change in current between adjacent points is minimum. Note that the selected arrangement of coils is scalable: more coils can be added so that

Section/Current	Section I	Section II	Section III	Section IV	Section V	Section VI
I_1	I_1^*	I_1^*	I_{2xy}^*	I_{3xy}^*	I_{2xy}^*	I_{3xy}^*
I_{2xy}	I_{2xy}^*	I_{3xy}^*	I_1^*	I_1^*	I_{3xy}^*	I_{2xy}^*
I_{3xy}	I_{3xy}^*	I_{2xy}^*	I_{3xy}^*	I_{2xy}^*	I_1^*	I_1^*

TABLE I

THE CURRENTS I_1, I_2 AND I_3 TAKE DIFFERENT VALUES DEPENDING ON THE SECTION WHERE WE WANT TO CREATE STATIC EQUILIBRIUM POINTS. ONCE THE DESIRED POSITION IS REFERRED TO SECTION I, THE CORRESPONDING VALUES OF CURRENT SHOWN MUST BE APPLIED.

the area where stable static equilibrium points can be created increases. To control a single microrobot, only 3 coils have to be powered at a given time to create equilibrium points at the desired positions, no matter the location on the arrangement or the size of it.

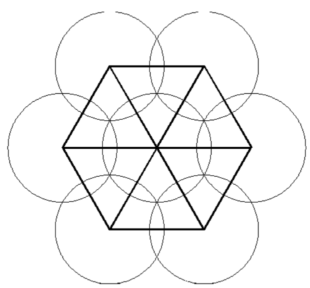

Fig. 8. A hexagonal area to control the microrobot using 7 coils.

The strategy to control the motion of a microrobot consists on creating equilibrium points close to the position of the microrobot in order to steer it in the desired direction. Since the equilibrium points are stable, the microrobot is guaranteed to move towards them: the motion of the microrobot can be controlled by creating sequences of equilibrium points describing the desired path.

IV. OPEN LOOP SIMULATIONS AND RESULTS

An arrangement of three coils in the corners of an equilateral triangle inscribed in a circle of radius $R = 25\,\mathrm{mm}$ was simulated. I_1^* was set to $0.02\,\mathrm{A}$, and the distance from the coils to the plane of the microrobot was set to $z_c = 0.02\,\mathrm{m}$. The dynamics of the microrobot were assumed to be first order dynamics of the form $\dot{\mathbf{x}} = k\mathbf{F}$, where $\mathbf{x}$ is the position vector of the microrobot, $\mathbf{F}$ is the vector of forces on the plane acting on the microrobot, and k was set to 10000.

Fig. 9 and Fig. 10 show the microrobot with initial position at the top vertex of the triangle following a circular path with desired entrance position at the right of the circle. Note that the path goes over all the sections of the triangle. The red circles are the successive static equilibrium points created to drive the robot, whose path is displayed in blue. Fig 10 shows how the particle goes from equilibrium point to equilibrium point following the vector field of each equilibrium.

Fig. 11 and Fig. 12 show the robot following a sinusoidal path with increasing amplitude, again crossing through all the sections of the triangle. In Fig. 11 the equilibrium points were created with an increasing separation from one another.

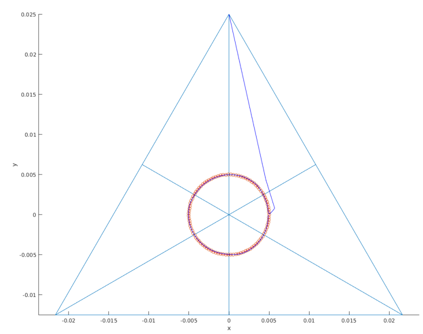

Fig. 9. Microrobot following a circular path.

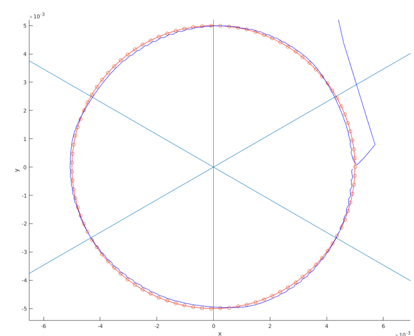

Fig. 10. Zoom in of a microrobot following a circular path.

Since the field created around each equilibrium point does not necessarily drives the robot in a straight line towards the equilibrium, the robot may stray away from the desired path. To correct this, equilibrium points closer to one another can be created, as shown in Fig. 12.

V. CONCLUSION AND FUTURE WORK

As future work, and immediate goal will be to proceed with experiments to test the algorithm, together with a control system capable of creating an equilibrium point in the desired position, without having obtained the current values experimentally previously. In lieu of a stable static equilibrium point sensor, visual feedback shall be used. The interpolation of currents from measured currents and positions giving stable static equilibria should be studied. Also, the posibility of controlling more than one microrobot will be explored.

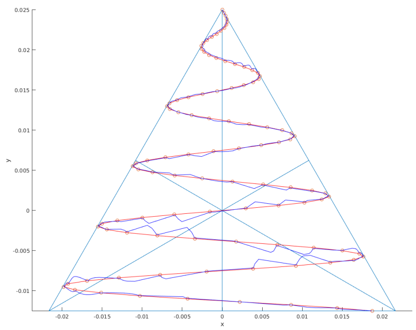

Fig. 11. Microrobot following a sinusoidal path.

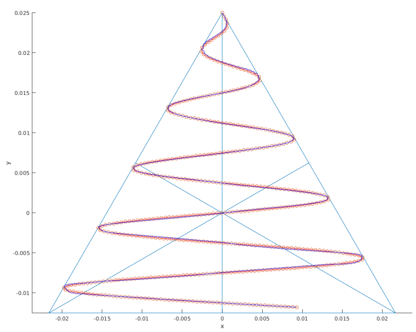

Fig. 12. Microrobot following a sinusoidal path with equilibrium points closer to each other.

REFERENCES

[1] A Becker, G Habibi, J Werfel, M Rubenstein, and J McLurkin. Massive uniform manipulation: Controlling large populations of simple robots with a common input signal. *IEEE Intl. Conf. on Intelligent Robots and Systems*, pages 520–527, 2013.

[2] Sagar Chowdhury, Wuming Jing, and DavidJ. Cappelleri. Controlling multiple microrobots: recent progress and future challenges. *Journal of Micro-Bio Robotics*, pages 1–11, 2015.

[3] Adelaide. Denis. A Discussion of the Cases When Two Quadratic Equations Involving Two Variables Can Be Solved by the Method of Quadratics. *The American Mathematical Monthly*, 94(8/9):192–199, 1903.

[4] Tara D. Edwards and Michael A. Bevan. Controlling colloidal particles with electric fields. *Langmuir*, 30(36):10793–10803, 2014. PMID: 24601635.

[5] Fischer, P and A Ghosh. Magnetically actuated propulsion at low Reynolds number: towards nanoscale control. *Nanoscale*, 3:557–563, 2011.

[6] D.J. Griffiths. *Introduction to Electrodynamics*. Prentice Hall, 1999.

[7] Wuming Jing, Xi Chen, Sean Lyttle, Zhenbo Fu, Yong Shi, and David J Cappelleri. Design of a micro-scale magnetostrictive asymmetric thin film bimorph (μmab) microrobot. In *ASME 2010 International Mechanical Engineering Congress and Exposition*, pages 599–607, 2010.

[8] I. S. M. Khalil, V. Magdanz, S. Sanchez, O. G. Schmidt, L. Abelmann, and S. Misra. Magnetic control of potential microrobotic drug delivery systems: Nanoparticles, magnetotactic bacteria and self-propelled microjets. In *Engineering in Medicine and Biology Society (EMBC), 2013 35th Annual International Conference of the IEEE*, pages 5299–5302, July 2013.

[9] Islam S. M. Khalil, Frank van den Brink, Ozlem Sardan Sukas, and Sarthak Misra. Microassembly using a cluster of paramagnetic microparticles. pages 5527–5532, 2013.

[10] H. Kim and M. J. Kim. Electric field control of bacteria-powered microrobots using a static obstacle avoidance algorithm. *IEEE Transactions on Robotics*, 32(1):125–137, Feb 2016.

[11] Michael P Kummer, Jake J Abbott, Bradley E Kratochvil, Ruedi Borer, Ali Sengul, and Bradley J Nelson. Octomag: An electromagnetic system for 5-dof wireless micromanipulation. *IEEE Trans. on Robotics*, 26(6):1006–1017, 2010.

[12] Sylvain Martel, Charles C Tremblay, Serge Ngakeng, and Guillaume Langlois. Controlled manipulation and actuation of micro-objects with magnetotactic bacteria. *Applied Physics Letters*, 89(23):233904, 2006.

[13] C. Pawashe, S. Floyd, and M. Sitti. Modeling and Experimental Characterization of an Untethered Magnetic Micro-Robot. *Intl. J. of Robotics Research*, 28(8):1077–1094, July 2009.

[14] Mahmut Selman Sakar, Edward B Steager, Dal Hyung Kim, A Agung Julius, MinJun Kim, Vijay Kumar, and George J Pappas. Modeling, control and experimental characterization of microbiorobots. *Intl. J. of Robotics Research*, 30(6):647–658, 2011.

[15] Edward B Steager, Mahmut Selman Sakar, Dal Hyung Kim, Vijay Kumar, George J Pappas, and Min Jun Kim. Electrokinetic and optical control of bacterial microrobots. *Journal of Micromechanics and Microengineering*, 21(3):035001, 2011.

[16] Edward B Steager, Mahmut Selman Sakar, Ceridwen Magee, Monroe Kennedy, Anthony Cowley, and Vijay Kumar. Automated biomanipulation of single cells using magnetic microrobots. *Intl. J. of Robotics Research*, 32(3):346–359, 2013.